Accessibility of the Functional Groups of Chitosan Aerogel Probed by FT-IR-Monitored Deuteration

Romain Valentin,[†,§] Barbara Bonelli,[†] Edoardo Garrone,[†] Francesco Di Renzo,[*,‡] and Françoise Quignard[‡]

Dipartimento di Scienza dei Materiali e Ingegneria Chimica, Politecnico di Torino, C.so Duca degli Abruzzi 24, 10129 Torino, Italy, and Institut C. Gerhardt, Matériaux Avancés pour la Catalyse et la Santé, UMR 5253 CNRS-UM2-ENSCM-UM1, ENSCM, 8 rue de l'Ecole Normale, 34296 Montpellier Cedex 5, France

Received April 7, 2007; Revised Manuscript Received August 15, 2007

Transmission FT-IR spectroscopy allowed us to monitor the deuteration of wafers of chitosan aerogel and xerogel by D_2O vapor at room temperature. The complete deuteration of the alcohol and amine groups of the aerogel (surface area 175 $m^2\ g^{-1}$ as measured by N_2 volumetry) confirmed the high accessibility of the functional groups of the polymer. The xerogel (surface area 5 $m^2\ g^{-1}$) was only partially deuterated in more severe conditions. The isotopic shift of the deuterated groups allowed us to confirm or revise some attributions of infrared bands of chitosan.

Introduction

The interest for chitosan (poly-β-(1,4)-glucosamine) stems from its applications in biomaterials, drug-delivery systems,[1−3] food additives, water clarification,[4] and as support for cells, enzymes,[5] and catalysts.[6] It is cheaply obtained by deacetylation of chitin wastes from the seafood industry. Most infrared spectroscopic studies of chitosan were aimed at the determination of the deacetylation degree of the chitin-derived materials[7−15] or were directed to the characterization of the polysaccharide in hybrid materials.[16−19] Albeit these works provided a sound vibrational characterization of the polymer, the preparation of the samples was unfit for the study of the reactivity of the functional groups by FT-IR spectroscopy of adsorbed probe molecules, a powerful technique widely applied to the study of inorganic solids or, less frequently, high-surface area polymers.[20−23] The wafers of dried polysaccharides used for former spectroscopic studies presented a very small surface area. As a consequence, a too small fraction of functional groups was accessible for a significant study of their interaction with probe molecules.

The aim of the present Article is to show the unique possibilities offered by supercritical drying to prepare chitosan samples in which a large fraction of amino groups is accessible. In the CO_2 supercritical extraction, the shrinkage induced by capillary evaporation is prevented, and the solid prepared in this way, known as an aerogel, retains a high degree of dispersion. Indeed, very high surface areas have been reported for polysaccharide aerogels: values close to 300 $m^2\ g^{-1}$ for alginate aerogels[24] and higher than 100 $m^2\ g^{-1}$ for chitosan aerogels.[25] Because of such a high dispersion of the polysaccharide, a large fraction of the functional groups are accessible to probe molecules.[25,26]

In this work, the accessibility of the functional groups of chitosan films has been monitored by FT-IR spectroscopy. The deuteration of the polysaccharide functional groups by D_2O vapors has been used as a probe reaction, and the isotopic shifts of the hydroxyl and amine bands have allowed us to improve the interpretation of the IR spectra.

Materials and Methods

Samples Preparation. Chitosan (from squid pen, Mahtani Chitosan PVT Ltd.) characterized by a degree of acetylation (DA) lower than 1.5% (measured by NMR and IR spectroscopy)[8,13] and a weight-average molecular weight of 200 000 g/mol (measured by size exclusion chromatography (SEC) coupled online with a multi-angle laser light scattering (MALLS) detector) was purified as follows: the polymer was dissolved at 1% (w/w) in a stoichiometric amount of aqueous acetic acid. After complete dissolution, it was filtered successively on 3, 1.2, 0.8, 0.45, and 0.2 μm cellulose ester membranes (Millipore). Chitosan was precipitated with diluted ammonia up to a constant pH 9 of the solution and separated by centrifugation. The precipitate was repeatedly washed with deionized water and centrifugated until a neutral pH was achieved, and then it was freeze-dried.

An aqueous solution was obtained by dissolving 0.2 g of purified chitosan in 10 mL of 0.055 M solution of acetic acid. This solution was spread out at room temperature in a Petri dish and gently covered by a 4 M NaOH solution. The gel was stored in the alkaline solution for 2 h and then filtered and washed with deionized water until pH 7.

Hydrogel Drying. Xerogel films were obtained after drying the hydrogel on glass plates in an oven at 323 K. To obtain the aerogel films, intermediate alcogels were formed by immersion of the hydrogel films in a series of successive ethanol−water baths of increasing alcohol concentration (10%, 30%, 50%, 70%, 90%, and 100%) during 15 min each. The aerogel films were obtained by drying the alcogels beyond the critical point of CO_2 (304.14 K, 738 MPa) in a Polaron 3100 apparatus. Reference cryogels were obtained by freezing the hydrogel films at 77 K and sublimating the ice under vacuum.

Evaluation of Textural Properties. Nitrogen adsorption/desorption isotherms were recorded in a Micromeritics ASAP 2010 apparatus at 77 K after outgassing the sample at 323 K under vacuum until a stable 3×10^{-3} mbar pressure was obtained with no more pumping. The surface areas were evaluated by the BET method. The average size of the polysaccharide fibrils was evaluated from the surface area by the formula $D = 4/(\rho S)$, where D is the fibril diameter in μm, S is the

* Corresponding author. Tel.: + 33 607508148. Fax: + 33 467163470. E-mail: direnzo@enscm.fr.
† Politecnico di Torino.
‡ ENSCM.
§ Present address: INRA BIA, BP 71627, 44316 Nantes, France.

10.1021/bm070391a CCC: $37.00
Published on Web 10/02/2007

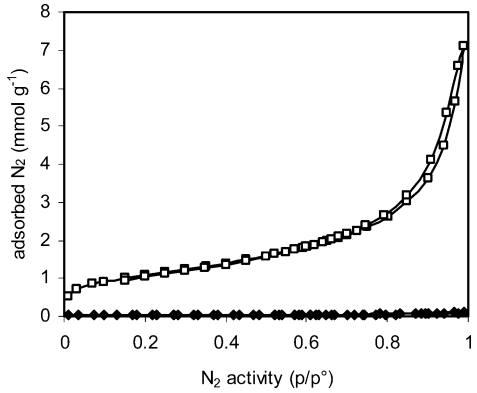

Figure 1. N_2 adsorption isotherms of a chitosan aerogel (□) and a chitosan cryogel (◆).

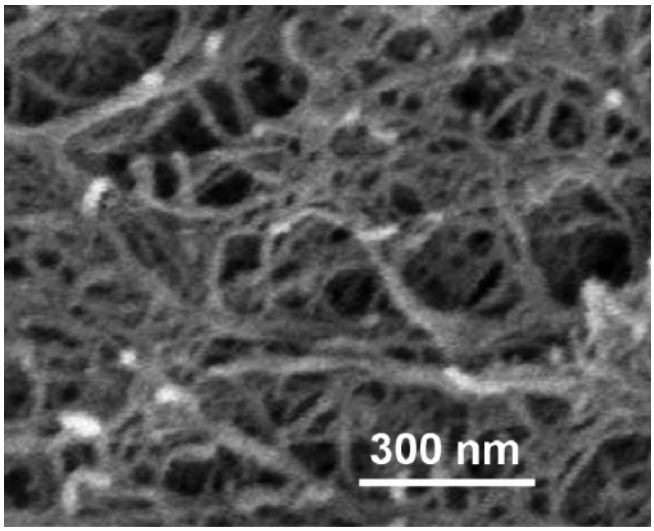

Figure 2. SEM picture of a chitosan aerogel.

surface area in $m^2\ g^{-1}$, and ρ is the volumic mass of chitosan in g/cm^3. The surface/volume ratio allows us to evaluate the fraction of geometrically exposed monomers. For these calculations, the material was assumed to present the properties ascertained for crystalline chitosan, a volumic mass of 1.23 g cm^{-3}, an area per monomer of 0.439 nm^2, and a volume per monomer of 0.196 nm^3.[20] Scanning electron micrographs (SEM) were recorded on a Hitachi S-4500 apparatus after platinum metallization.

Infrared Spectroscopy. Suitable wafers were cut from the chitosan films and placed into an all-silica cell provided with KBr windows for transmission IR measurements. The wafers were supported by a gold case. The cell allowed evacuation, heat treatment, and pressure measurement. FT-IR spectra were recorded on a Bruker Vector 22 spectrometer, equipped with an MCT detector. The spectral resolution was 2 cm^{-1}, and 36 scans were registered for each spectrum. Adsorption of D_2O was carried out on wafers evacuated in situ at 353 K (residual pressure lower than 10^{-6} mbar). Successive pulses of D_2O vapor were introduced in the cell, and measurement was performed after pressure equilibrium was reached after each introduction of D_2O. In the case of adsorption on the xerogel sample, measurements were performed 30 min after each introduction of D_2O.

Results and Discussion

Textural Properties of the Materials. For the purpose of this Article, a xerogel is defined as a dried gel that has considerably shrinked during drying. An aerogel is instead a dried gel that has retained most porous volume of the parent hydrogel.[21] Drying a hydrogel can result in a xerogel or an aerogel according to the drying method used. When the solvent, usually water, is evaporated, the capillary tension at the vapor−liquid interface brings together the secondary units of the gel. As a consequence, a xerogel with low porosity is formed. Alternatively, the solvent can be exchanged with a secondary solvent, usually CO_2 or low-molecular weight hydrocarbons, which is in turn compressed and heated beyond its critical point and evacuated as a supercritical fluid, in conditions in which no gas−liquid interface exists. In this way, the supercritical drying avoids the drawbacks related to capillary tension and prevents the pores of the material from collapsing. The aerogel formed retains in the dry state an image of the dispersion of the wet gel.

Several previous spectroscopic studies on polysaccharide gels have been carried out on cryogels produced by freeze-drying. The ice formed by freezing the solvent can be sublimated with no capillary tension, and most of the volume of the hydrogel can be retained. However, the pressure of growing ice crystals can significantly alter the internal structure of the gel during freezing, if the size of the sample and the conditions of cooling are not in an optimal range.[29,30] A possible result is the collapse of the local porosity despite the preservation of the total volume of the gel.

The adsorption−desorption isotherms of N_2 at 77 K on an aerogel and a cryogel of chitosan are reported in Figure 1. The isotherm on the supercritical-dried aerogel is at the borderline between type II and type IV according to the IUPAC classification,[31] corresponding to a macroporous adsorbent (pores with diameter larger than 50 nm) with a small contribution of mesoporosity (pores with diameter between 2 and 50 nm). The surface area of the aerogel is 175 $m^2\ g^{-1}$. Such a surface area corresponds to an average diameter of the chitosan fibrils of 18 nm and indicates that nearly 10% monomers are exposed at the surface. The scanning electron microscopy of the chitosan aerogel, whose picture is reported in Figure 2, shows an open network of fibrils with a size consistent with the diameter evaluated by the adsorption data.

Figure 1 clearly shows that a much lower amount of N_2 is adsorbed on the chitosan cryogel. The surface area of the cryogel, as measured by N_2 adsorption at 77 K, is 5 $m^2\ g^{-1}$, the same value measured for the evaporatively dried xerogel. This value of surface area corresponds to an average diameter of the chitosan fibers about 0.7 μm and indicates that less than 0.3% monomers are exposed at the surface.

On the basis of their respective degree of dispersion, it can be expected that deuteration reactions would be more hindered by diffusion in the case of the xerogel than in the case of the aerogel.

Deuteration of the Aerogel. The IR spectra of the outgassed aerogel before and after exposal to doses of D_2O vapor are reported in Figure 3 from 3800 to 1800 cm^{-1} and in Figure 4 from 1800 to 600 cm^{-1}.

The O−H and N−H stretching bands form a broad envelope with main bands at wavenumbers around 3435, 3290, and 3180 cm^{-1}. The queue of the envelope toward lower wavenumbers extends until 2500 cm^{-1}, indicating a high level of hydrogen bonding of the functional groups. Significant bands of gaseous CO_2 correspond to unbalancing of the background magnified by the saturation of the signal.

The admission of D_2O vapor brings about a progressive decrease of the intensity of all O−H and N−H bands. At a D_2O pressure of 13 mbar, the O−H and N−H bands have virtually disappeared, indicating a nearly complete deuteration of the alcohol and amine groups of the aerogel. The residual

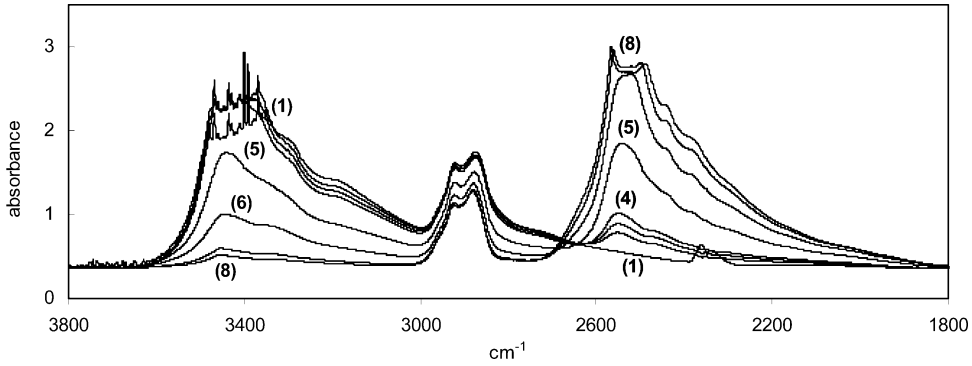

Figure 3. IR spectra of chitosan aerogel outgassed at 353 K (1) and exposed to D_2O pressure of 0.01 (2), 0.24 (3), 0.33 (4), 3.7 (5), 9.7 (6), 12 (7), and 13 (8) mbar. Wavenumber domain 3800−1800 cm^{-1}.

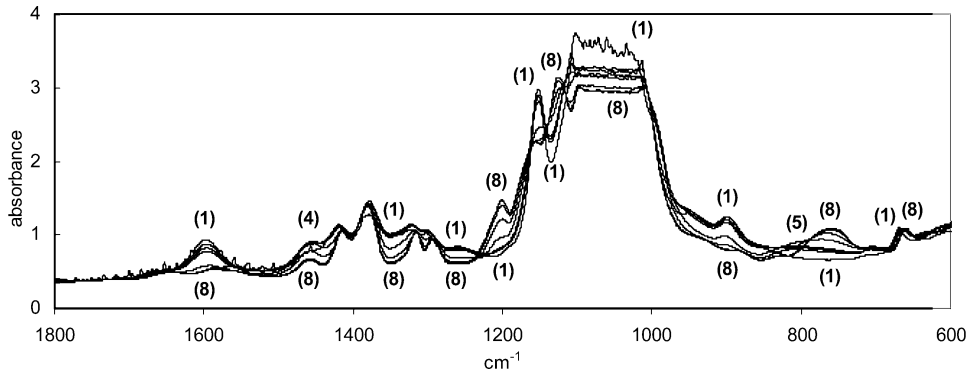

Figure 4. IR spectra of chitosan aerogel outgassed at 353 K (1) and exposed to D_2O pressure of 0.01 (2), 0.24 (3), 0.33 (4), 3.7 (5), 9.7 (6), 12 (7), and 13 (8) mbar. Wavenumber domain 1800−600 cm^{-1}.

intensity at 3435 cm^{-1} corresponds to less than 0.5% residual OH groups. As the geometry of the chitosan fibrils suggests that no more than 10% monomers are at the surface of the fibrils, this degree of isotopic exchange indicates that D_2O can penetrate for several nanometers inside the polymer.

In close parallel with the decrease of the absorbance of the proton-bearing groups, the bands of the deuterated groups appear and grow at wavenumbers with maxima at 2529, 2432, and 2372 cm^{-1}. The isotopic shifts corresponds to a ratio $r_{exp} = \nu(O-H)/\nu(O-D) = 1.358$, somewhat short of the ratio $r_{red} = \nu(O-H)/\nu(O-D) = 1.3744$ expected after the variation of reduced masses between protonated and deuterated species. This difference is probably related to the anharmonicity of the stretch of the hydroxyl bond. In the case of the isolated silanol group on silica, as well as of the O−H bridged species in zeolites, Kustov et al. have shown, by measuring several overtones, that the O−H stretching vibration is well represented by a Morse potential. Moreover, the anharmonicity parameter is also practically the same in both cases.[32,33] Assuming this same value of the anharmonicity parameter also for the present case of chitosan brings about an isotopic shift $r_{anharn} = \nu(O-H)/\nu(O-D) = 1.355$, in very good agreement with the experimental value measured on chitosan.

It can be observed that the envelope of the protonated groups, when allowance is made for spectra saturation, retains the same overall shape at all levels of deuteration. In the same way, the relative intensities of the bands of the deuterated groups remain the same during their rise of intensity. The homothetical variation of the absorbance of the alcohol and amine bands indicates that D_2O is such an effective deuterating agent that no differences can be observed among the reactivities of the O−H and N−H groups.

The C−H stretching vibrations at 2914 and 2865 cm^{-1} are unaffected by deuteration, as expected on the basis of the low reactivity of the aliphatic C−H bonds.

The IR spectra in the wavenumber domain 1800−600 cm^{-1} for the aerogel, outgassed and exposed to doses of D_2O vapor, are reported in Figure 4. The NH_2 scissoring mode of the primary amine is observed at 1593 cm^{-1}, and the very low intensity of the amide band at 1655 cm^{-1} indicates a high degree of deacetylation of the sample.

The NH_2 scissoring band at 1593 cm^{-1} disappears with deuteration. The isotopic shift of this vibration has been calculated for other amines and allows us to attribute to ND_2 scissoring the band that appears at 1197 cm^{-1}.[34,35] It has to be observed that the rise of the band of the deuterated group does not exactly mirror the decrease of the band of the protonated group. The NH_2 scissoring band has virtually disappeared when the sample is at the equilibrium with less than 4 mbar D_2O vapor, whereas the ND_2 scissoring band is just appearing at such a pressure and grows at higher D_2O pressure. This trend suggests the presence of an intermediate NHD group, whose bending wavenumber should be intermediate between the wavenumbers of the NH_2 and ND_2 bands. It can be observed that the absorbance at 1453 cm^{-1} increases when the D_2O pressure rises until 3.7 mbar and decreases when the D_2O pressure increases further.

The band at 1453 cm^{-1} also includes a component whose intensity is not affected by isotopic exchange and which can be attributed to CH_2 scissoring. The intensity of the band at 1376 cm^{-1} is virtually unaffected by the isotopic exchange. This allows us to discard its attribution to a C−OH stretching mode.[19] The attribution to the C−H bending of the methyne group is more likely, possibly with a contribution of CH_2 wagging.[7,34] The bands at 1414, 1319, and 1295 cm^{-1} can be attributed to

Table 1. Main IR Bands of Chitosan and Deuterated Chitosan

	wavenumber (cm^{-1})	
mode	chitosan	O-, N-deuterated chitosan
O−H stretching	3435	2529
N−H stretching	3290, 3180	2432, 2372
C−H stretching	2914, 2865	2914, 2865
NH_2 scissoring	1593	1197
CH_2 scissoring	1453	1453
CH_2 bending	1414	1412
CH bending, CH_2 wagging	1376	1376
CH_2 twisting	1319, 1295	1312, 1289
O−H bend, NH_2 twist	1254	?
C−OH stretching	1150	1121
C−O, C−N, CC stretching	1100−1000	1100−1000
NH_2 wagging	950, 898	760
O−H out-of-plane bending	668	658

CH_2 bending or twisting modes.[7,17,33] These bands underwent an isotopic shift of some wavenumbers with no significant change of intensity with deuteration. This effect, observed in other instances, is an example of the way in which relatively distant substituents can affect the frequency of infrared vibrations.[34]

The absorbance around 1345 and 1260 cm^{-1} strongly decreases with deuteration. Among the vibrations whose intensity can be strongly affected by the isotopic exchange, O−H in-plane bending or NH_2 twisting modes would be compatible with these wavenumbers.[35,36] An ultimate attribution of these bands, as well as of the C−H bending bands, would demand the complete modelization of the fundamental frequencies of chitosan.

The band at 1150 cm^{-1} has been differently attributed to the asymmetric stretching mode of the C−OC glycosidic bond or to the C−OH stretching of the secondary alcohol groups.[7,18] The second interpretation has surely to be retained on the basis of the strong isotopic shift of the band. The difference of the reduced masses of the OH and OD groups allows us to attribute to the corresponding C−OD stretching the band that appears at 1121 cm^{-1}, beyond a clear isosbestic point.

Strong C−O, C−N, and C−C stretching vibrations dominate the region between 1100 and 1000 cm^{-1}.

The intensity of the bands at 950 and 898 cm^{-1} rapidly decreases when D_2O vapors are admitted, and they virtually disappear at high D_2O pressure. These bands have been attributed to, respectively, $C-CH_3$ wagging and ring stretching modes.[7] Such modes would not be affected by isotopic effects, and, if they are present, they are overwhelmed by strong isotope-sensitive modes. NH_2 wagging vibrations are expected at these wavenumbers on the basis of calculations of other amines.[34,35] The corresponding ND_2 wagging vibrations have been calculated at wavenumbers compatible with a very broad band that appears and grows with deuteration around 760 cm^{-1}.[34,35] At intermediate wavelengths around 810 cm^{-1}, the absorbance increases with D_2O pressure up to 3.7 mbar and decreases for further pressure rise, possibly in correspondence with a NHD wagging vibration.

A significant isotopic shift, from 668 to 658 cm^{-1}, is also observed for a band that can be attributed to O−H out-of-plane bending.[7,36]

For ease of consultation, the attributions of the main IR bands of chitosan and deuterated chitosan are reported in Table 1.

Deuteration of the Xerogel. The IR spectra of the outgassed xerogel before and after exposal to doses of D_2O vapor are reported in Figure 5, from 3800 to 1800 cm^{-1}, and Figure 6, from 1800 to 400 cm^{-1}. The spectrum of the outgassed xerogel is nearly indistinguishable from the spectrum of the outgassed aerogel. However, its modifications upon exposure to D_2O vapors are much less intense. Exposal to 17 mbar D_2O (curve

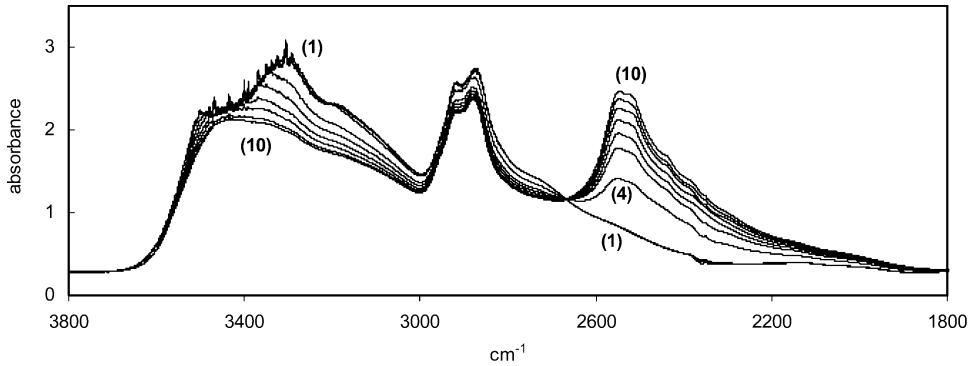

Figure 5. IR spectra of chitosan xerogel outgassed at 353 K (1) and exposed to D_2O pressure of 0.14 (2), 1.3 (3), and 17 (4) mbar and at repeated cycles of evacuation and exposure to 17 mbar D_2O (5−10). Wavenumber domain 3800−1800 cm^{-1}.

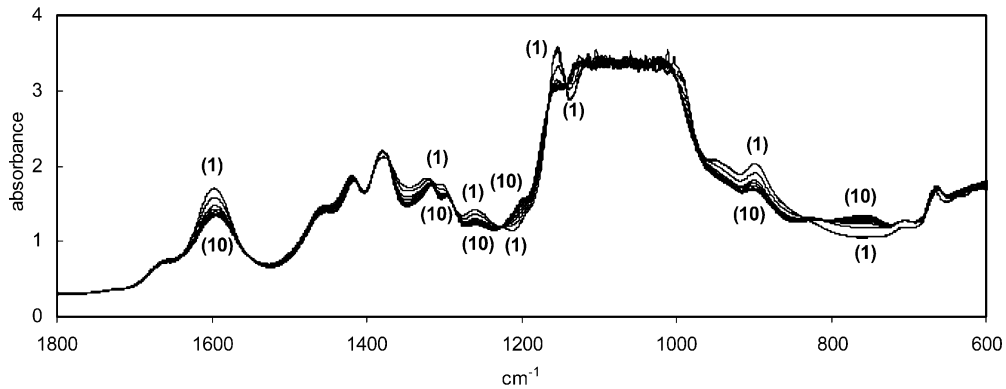

Figure 6. IR spectra of chitosan xerogel outgassed at 353 K (1) and exposed to D_2O pressure of 0.14 (2), 1.3 (3), and 17 (4) mbar and at repeated cycles of evacuation and exposure to 17 mbar D_2O (5−10). Wavenumber domain 1800−600 cm^{-1}.

4 in Figure 4) brought about a very limited formation of O−D and N−D groups, as visible in the 2600−2200 cm^{-1} region.

Several cycles of outgassing and admission of D_2O at the same pressure (17 mbar) were needed to move further toward the equilibrium of isotopic exchange (curves 5−10 in Figure 5). Nevertheless, the decrease of the O−H and N−H stretching bands and the growth of the O−D and N−D stretching bands were much more limited than in the case of the aerogel, and the isotopic exchange was far from complete. It can be observed that a limited degree of isotopic exchange was also achieved in the pioneering experiments of chitin deuteration by Pearson and co-workers.[7]

The shapes of the envelopes of bands corresponding to protonated and deuterated species are very similar in the xerogel and the aerogel. It seems likely that a surface rim of the xerogel is completely exchanged and that the diffusion of D_2O inside the xerogel demands a longer time than the duration allotted to the IR experiment.

The low accessibility of the xerogel to the deuterating agent is confirmed by the examination of the lower-wavenumber part of the spectra, reported in Figure 6. Albeit most of the characteristic effects of deuteration observed in the spectra of the aerogel can be identified in the spectra of the xerogel, all of them correspond to partial transformations. The evolution of the NH_2 scissoring mode at 1593 cm^{-1} and the corresponding ND_2 scissoring at 1197 cm^{-1}, as well as the evolution of the NH_2 wagging at 950 and 898 cm^{-1} and the ND_2 wagging around 760 cm^{-1}, indicates a partial deuteration of the amine group. In the same way, the evolution of the alcoholic C−O stretching at 1150 cm^{-1} confirms a partial deuteration of the alcohol groups.

A significant feature of the spectra of the xerogel as well as of the aerogel is the very limited contribution of the bands of molecular D_2O or H_2O. Only a shoulder at 2510 cm^{-1} could be attributed to adsorbed molecular D_2O. Considering that the activity of D_2O at 17 mbar and 398 K is nearly 0.7, the adsorption of molecular water appears to be very low and supports the observation of a hydrophobic character of the chitosan fibrils.[37,38]

Conclusions

The different reactivity of organic groups toward deuteration represents a useful tool for the identification of the spectral vibrations. The isotopic exchange of deuterium for hydrogen in alcohol or amine groups allows us to differentiate them from the less reactive C−H groups or from the unreactive C−O−C or C−C bonds.

Moreover, the extent of isotopic exchange allows us to evaluate the accessibility of the material to the deuterating agent. Under this respect, the aerogel and xerogel of chitosan differ in a striking manner. While the aerogel can be easily and completely deuterated by exposal to D_2O vapors, the xerogel can only be partially deuterated in more severe conditions. In this way, the deuterating agent is a probe of the accessibility of the materials to small polar molecules, and the difference observed indicates at which point the chitosan aerogel can be more effective than a xerogel for applications in catalysis or adsorption.

Acknowledgment. We thank Didier Cot for assistance with scanning electron microscopy.

References and Notes

(1) Gerentesa, P.; Vachoud, L.; Dourya, J.; Domard, A. *Biomaterials* **2002**, *23*, 1295.
(2) Sinha, V. R.; Singla, A. K.; Wadhawan, S.; Kaushik, R.; Kumria, R.; Bansal, K.; Dhawan, S. *Int. J. Pharm.* **2004**, *274*, 1.
(3) Ravi Kumar, M. N. V.; Muzzarelli, R. A. A.; Muzzarelli, C.; Sashiwa, H.; Domb, A. J. *Chem. Rev.* **2004**, *104*, 6017.
(4) Winterowd, J. G.; Sandford, P. A. In *Food Polysaccharides and their Applications*; Stephen, A. M., Ed.; Marcel Dekker: New York, 1995; p 441.
(5) Dumitriu, S.; Chornet, E. In *Polysaccharides*; Dumitriu, S., Ed.; Marcel Dekker: New York, 1998; p 629.
(6) Guibal, E. *Prog. Polym. Sci.* **2005**, *30*, 71.
(7) Pearson, F. G.; Marchessault, R. H.; Liang, C. Y. *J. Polym. Sci.* **1960**, *18*, 101.
(8) Sannan, T.; Kurita, K.; Ogura, K.; Iwakura, Y. *Polymer* **1978**, *19*, 458.
(9) Moore, G. K.; Roberts, G. A. F. *Int. J. Biol. Macromol.* **1980**, *2*, 115.
(10) Miya, M.; Iwamoto, R.; Yeshikawa, S.; Mima, S. *Int. J. Biol. Macromol.* **1980**, *2*, 323.
(11) Domard, A. *Int. J. Biol. Macromol*. **1987**, *9*, 333.
(12) Baxter, A.; Dillon, M.; Taylor, K. D. A.; Roberts, G. A. F. *Int. J. Biol. Macromol.* **1992**, *14*, 166.
(13) Shigemasa, Y.; Matsuura, H.; Sashiwa, H.; Saimoto, H. *Int. J. Biol. Macromol*. **1996**, *18*, 237.
(14) Brugnerotto, J.; Lizardi, J.; Goycoolea, F. M.; Argüelles-Monal, W.; Desbrières, J.; Rinaudo, M. *Polymer* **2001**, *42*, 3569.
(15) Duarte, M. L.; Ferreira, M. C.; Marvão, M. R.; Rocha, J. *Int. J. Biol. Macromol.* **2002**, *31*, 1.
(16) Qu, X.; Wirsén, A.; Albertsson, A. C. *J. Appl. Polym. Sci.* **1999**, *74*, 3186.
(17) Pawlak, A.; Mucha, M. *Thermochim. Acta* **2003**, *396*, 153.
(18) Wang, T.; Turhan, M.; Gunasekaran, S. *Polym. Int.* **2004**, *53*, 911.
(19) Saraswathy, J.; Pal, S.; Rose, C.; Sastry, T. P. *Bull. Mater. Sci. Indian Acad. Sci.* **2001**, *24*, 415.
(20) Ryczowski, J. *Catal. Today* **2001**, *68*, 263.
(21) Knözinger, H.; Huber, S. *J. Chem. Soc., Faraday Trans.* **1998**, *94*, 2047.
(22) Buzzoni, R.; Bordiga, S.; Ricchiardi, G.; Spoto, G.; Zecchina, A. *J. Phys. Chem.* **1995**, *99*, 11937.
(23) Zecchina, A.; Spoto, G.; Bordiga, S. *Phys. Chem. Chem. Phys*. **2005**, *7*, 1627.
(24) Valentin, R.; Molvinger, K.; Quignard, F.; Di Renzo, F. *Macromol. Symp.* **2005**, *222*, 93.
(25) Valentin, R.; Molvinger, K.; Quignard, F.; Brunel, D. *New J. Chem*. **2003**, *27*, 1690.
(26) Valentin, R.; Horga, R.; Bonelli, B.; Garrone, E.; Di Renzo, F.; Quignard, F. *Biomacromolecules* **2006**, *7*, 877.
(27) Ogawa, K.; Yui, T.; Okuyama, K. *Int. J. Biol. Macromol.* **2004**, *34*, 1.
(28) Pierre, A.; Pajonk, G. *Chem. Rev.* **2002**, *102*, 4243.
(29) Kocklenberg, R.; Mathieu, B.; Blacher, S.; Pirard, R.; Pirard, J. P.; Sobry, R.; Van den Bossche, G. *J. Non-Cryst. Solids* **1998**, *225*, 8.
(30) Serp, D.; Mueller, M.; von Stockar, U.; Marison, I. W. *Biotechnol. Bioeng.* **2002**, *79*, 243.
(31) Rouquerol, F.; Rouquerol, J.; Sing, K. *Adsorption by Powders and Porous Solids*; Academic Press: San Diego, 1999; p 18.
(32) Kustov, L. M.; Borovkov, V. Yu.; Kazansky, V. B. *J. Catal.* **1981**, *72*, 149.
(33) Ugliengo, P.; Garrone, E. *J. Mol. Catal.* **1989**, *54*, 439.
(34) Giorgini, M. G.; Pelletti, M. R.; Paliani, G.; Cataliotti, R. S. *J. Raman Spectrosc*. **1983**, *14*, 16.
(35) de Carvalho, L. A. E. B.; Lourenço, L. E.; Marques, M. P. M. *J. Mol. Struct.* **1999**, *482*, 639.
(36) Coates, J. In *Encyclopedia of Analytical Chemistry*; Meyers, R. A., Ed.; Wiley: Chichester 2000; p 10815.
(37) Montembault, A.; Viton, C.; Domard, A. *Biomaterials* **2005**, *26*, 933.
(38) Boucard, N.; David, L.; Rochas, C.; Montembault, A.; Viton, C.; Domard, A. *Biomacromolecules* **2007**, *8*, 1209.

BM070391A